Determination of Mass Transfer Coefficients for Bubble-Free Devolatilization of Polymeric Solutions in Twin-Screw Extruders

Theoretical and experimental studies have been conducted on the mass transfer rates which occur during the continuous devolatilization of bubble-free polymeric solutions in a corotating twin-screw extruder. Experimental measurements of the mass transfer rates, when reported in terms of the product of the individual liquid phase mass transfer coefficient and the surface area for mass transfer per unit volume of empty extruder, were found to correlate well with screw speed in accordance with the predictions of a model based on penetration theory. It is shown, however, that significant differences exist between the measured and predicted values for the rates of mass transfer, which leads to the conclusion that the surface area for mass transfer is substantially smaller than the value computed on the basis that continuous films are formed on the surfaces of the screws and the barrel wall.

G. P. COLLINS and C. D. DENSON

Department of Chemical Engineering
University of Delaware
Newark, DE 19711

G. ASTARITA

Istituto di Principi di
Ingegneria Chemica
Piazzale Tecchio
80125 Napoli, Italy

SCOPE

The removal of volatile components from polymeric solutions, commonly known as devolatilization, is a unit operation that finds importance in both the synthesis of polymers and the shaping of polymeric materials to form finished goods. Condensation polymerizations, for example, require that (volatile) by-products be continuously removed during polymerization so that reverse reactions will not prevent the formation of high molecular weight products (Odian, 1970). And, in food packaging applications which involve the use of polymeric materials, residual monomer must be reduced to levels of the order of parts per million since some of these monomer are thought to be carcinogenic (Todd, 1974; Hess and Eise, 1977).

In commercial practice when polymeric solutions of high viscosity are to be stripped of volatile components, the devolatilization operation is almost always conducted in geometries which generate a wiped film, and here single-screw extruders have played a major role. In recent years, increasing attention has been given to conducting these operations in twin-screw extruders, especially in circumstances when a chemical reaction is involved, and this has led to significant advances in the technology related to the use of these machines for stripping operations. As judged by the published literature, however, a scientific understanding of stripping operations in twin-screw extruders is far from complete, thereby bringing into question whether the engineering analysis and design of these processes can be performed in a rational manner and with confidence.

The research reported here was undertaken as a first step toward ultimately developing a more complete understanding of polymer devolatilization processes in twin-screw extruders. Mass transfer rates were determined experimentally at various liquid flow rates and screw speeds using a solvent-free inert gas at atmospheric pressure to strip a volatile component from a polymeric solution for which the diffusion coefficient and Henry's constant were known. These results are reported in terms of $k_L a$, the product of the individual liquid phase mass transfer coefficient and the surface area for mass transfer per unit volume of empty extruder. A theoretical expression for the liquid phase mass transfer coefficient was also developed using penetration theory. The results from this analysis are compared with the experimental results and the differences between the two are discussed in light of the model assumptions.

CONCLUSIONS AND SIGNIFICANCE

When bubble-free polymeric solutions are devolatilized in fully intermeshing, corotating twin-screw extruders, mass transfer occurs by molecular diffusion from the nip formed in the partially-filled channels of the screws and from the wiped films generated on the surface of the screws and the barrel wall. The rate at which mass is transferred during devolatilization

Correspondence concerning this paper should be addressed to C. D. Denson.
G. P. Collins is presently at Technical Center, Mobil Chemical Co., Macedon, NY 14502.

can be described in terms of a liquid phase mass transfer coefficient, an appropriate driving force, and the combined surface area of the wiped films and the nip. The mass transfer coefficient depends on the molecular diffusivity (a material property), the rotational speed of the screws (a process variable), the number of screw tips (an equipment variable), and the ratio of the distance between screw centers to the radius of the barrel (an equipment variable). Generally, the mass transfer coefficient is of the order of 10^{-6} m/s.

The surface areas of the wiped films on the screws and the barrel wall play a dominant role in the rate at which mass transfer occurs. But it appears that the surface areas which actually participate in the mass transfer process are substantially less than the surface areas that would be computed on the basis that the screws and the barrel wall are completely coated with the polymeric solution. The role that the intermeshing zone plays in the mass transfer process is not entirely clear; however, the fact that a model based on penetration theory predicts the correct dependence on screw speed suggests that the intermeshing zone provides additional mixing which results in a uniform concentration of the volatile component throughout the bulk prior to successive exposures to the vapor phase. This has the effect of maximizing the driving force for interphase mass transfer at the beginning of each exposure.

The significance of this work rests on its being the first reported study which unambiguously demonstrates that devolatilization rates for bubble-free polymeric solutions in twin-screw extruders can be described in tems of a liquid phase mass transfer coefficient. It is also significant in that it shows how mass transfer rates can be predicted from first principles provided there is some understanding concerning the nature of liquid polymric films formed on solid substrates. In view of the fact that the mass transfer coefficient is a well-established concept in the design procedures for stripping operations in the traditional chemical process industries, this work suggests that these same procedures would be applicable in the design of the unusual geometries encountered in the polymer processing industries.

INTRODUCTION

Unlike the case for single-screw extruders—where considerable research of a scientific and fundamental nature has been devoted to developing an engineering understanding of devolatilization (Latinen, 1962; Coughlin and Canevari, 1969; Roberts, 1970; Biesenberger, 1980)—little work of a similar nature has been conducted in relation to devolatilization in twin-screw extruders. With the exception of the work of Todd (1974) and Werner (1980), almost all of the published literature has dealt with the commercial application of twin extruders in the devolatilization of polymeric solutions.

Todd (1974) studied devolatilization at reduced pressures in an intermeshing, corotating twin-screw extruder using styrene-polystyrene and hexane-polyethylene systems. Exit concentrations of the volatile component were measured at various operating conditions and good agreement was found between these data and the predictions of what appears to be a semiempirical model that Todd developed. Insufficient detail is given in the published work concerning the experimental procedure and the assumptions underlying the model to determine whether the model is applicable to a broader range of materials systems and operating conditions. Werner (1980) describes several devolatilization processess that have been conducted in twin-screw extruders and shows typical data obtained from processes of commercial interest. Quantitative relations were developed on the basis of semiempirical considerations, and these appear to be useful in predicting extruder performance.

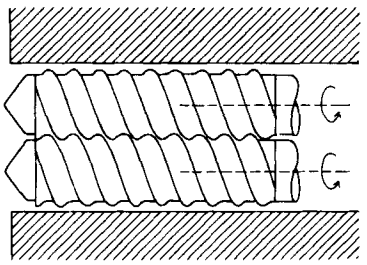

Figure 1. Fully intermeshing, self-wiping corotating twin-screw extruder.

BACKGROUND

Figure 1 shows a typical fully intermeshing corotating twin-screw extruder. These extruders are usually differentiated on the basis of the number of tips or starts that a screw element has. Figure 2 shows, for example, a two-tipped screw element of the type which will be considered in this work; the view is a cross section taken perpendicular to the barrel axis.

The restraint that the tip of one screw element wipe the flank of its mate leads to a unique relationship for the shape of the screw channel. Figure 3 is an isometric view of this channel and Figure 4 is a cross section of the channel in a plane perpendicular to the plane which defines the helix angle. This latter figure shows the actual shape of the channel which is described by the following expressions:

$$h(x) = H = 2R_s - C_L \quad 0 \le x \le \frac{e}{2} \tag{1}$$

$$h(x) = R_s \left\{ 1 + \cos \left[\frac{2\pi \left(x - \frac{e}{2} \right)}{t_s \cos\phi} \right] \right\}$$

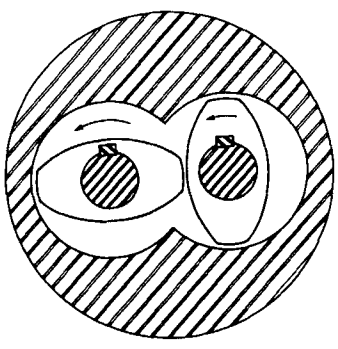

Figure 2. Cross section of a two-tipped intermeshing twin-screw extruder.

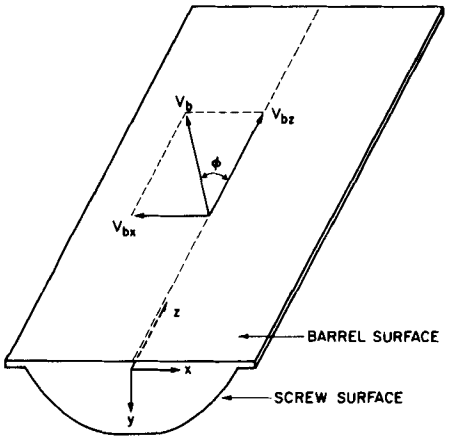

Figure 3. Isometric view of unwound channel of an intermeshing twin-screw extruder.

$$-\sqrt{C_L^2 - R_s^2 \sin^2\left[\frac{2\pi\left(x-\frac{e}{2}\right)}{t_s\cos\phi}\right]}\quad \frac{e}{2} \le x \le \frac{w}{2} \tag{2}$$

$$h(x) = 0 \quad \frac{W}{2} \le x \le \frac{W}{2} + \frac{e}{2}. \tag{3}$$

The quantities W, e, t_s are given by the following expressions:

$$W = \frac{t_s\cos\phi}{p} - e \tag{4}$$

$$t_s = \pi D_s \tan\phi \tag{5}$$

$$e = \frac{t_s\alpha\cos\phi}{2\pi} \tag{6}$$

$$\alpha = \frac{\pi}{p} - 2\cos^{-1}\frac{\rho_c}{2} \tag{7}$$

A more detailed description of the classification of twin-screw extruders and of the mathematical relationships which define the geometry is given by Hwang (1982).

In the devolatilization process the screw channels are partially filled with the polymeric solution to be stripped of the volatile component (see Figure 5); thus the remainder of the screw channel is available for the evaporated liquid. Because the barrel has a component of motion, V_{Bz}, in the down-channel direction, the solution is caused to flow from the extruder inlet to the outlet, which in this case is out of the plane of the paper. The cross-channel component of the barrel motion, V_{Bx}, has two effects. First, it causes a circulation of the fluid in the nip and because of the continual exposure of fresh material at the surface of the fluid in the

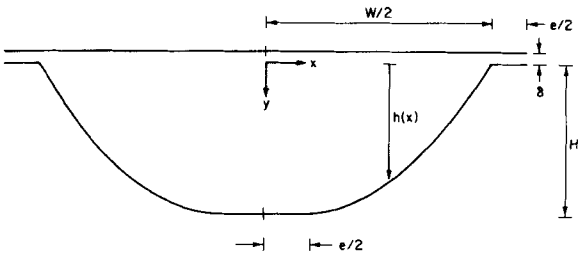

Figure 4. Channel profile and coordinate system of a screw element as viewed in the down-channel direction.

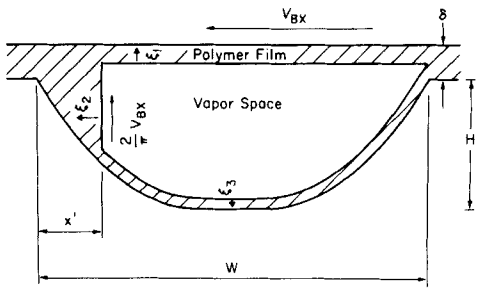

Figure 5. Schematic cross section of a partially filled channel showing polymer films, nip, and vapor space present during devolatilization.

nip, mass is transferred to the gas phase which contains the volatile component at a lower fugacity. On the basis of an analysis by Moffatt (1964), who showed that the velocity of an infinite free surface perpendicular to a moving wall is $2/\pi$ times the wall velocity, the velocity of fluid at the surface of the nip can be approximated as $(2/\pi)V_{Bx}$ and thus the exposure time for mass transfer is approximately given by

$$\theta_n = \frac{\pi}{2}\frac{h}{V_{Bx}} \tag{8}$$

The second effect which results from the cross-channel component of the barrel motion is to generate a wiped film of the polymeric solution as the solution is dragged from the nip in an adjacent screw channel through the clearance between the flight tip and the barrel. Since this film is continually generated, mass is transferred to the gas phase in a time period given by

$$\theta_f = \frac{W - x'}{V_{Bx}} \tag{9}$$

again, in circumstances when the fugacity of the volatile component in the gas phase is lower than that in the solution.

THEORY

On the basis of the simplified view of the flow patterns just described for flows in a twin-screw extruder, a model for predicting mass transfer rates can be developed using penetration theory and the fact that mass is transferred simultaneously from the nip, the wiped film on the barrel wall, and the wiped film on the screws which is generated by the self-wiping action of the screws. We can therefore write that the total molar mass transfer rate from an element of fluid over a length dz in the extruder is

$$N_t a S dz = (N_n a_n + N_f a_f + N_{fs} a_{fs}) S dz \tag{10}$$

a mass balance across the same differential element results in

$$\frac{d}{dz}(Lw) = -(N_n a_n + N_f a_f + N_{fs} a_{fs}) SM \tag{11}$$

Equation 11 can be solved to obtain a relationship between the extruder inlet and exit concentrations, the liquid flow rate, and the operating conditions once the mathematical form for the quantity in parentheses on the righthand side of Eq. 11 is known.

The development of a specific expression for the mass transfer rate in Eq. 11 is based on penetration theory and closely parallels the development by Latinen (1962), who was the first to show how penetration theory could be applied to the analysis of devolatilization in single screw extruders. In our use of penetration theory we shall make the following assumptions:

1. The diffusion coefficient is independent of concentration and temperature.
2. The penetration depth for diffusion is small compared to the thickness of the liquid layer.

3. The initial concentration of the volatile component in each of the wiped films is uniform and equal to the bulk concentration of the volatile component in the nip.

4. The concentration of the volatile component in the nip is uniform as a result of the material in the nip having passed through the intermeshing zone where the twin screws meet; this concentration is the initial concentration for mass transfer from the nip.

In view of the above assumptions, each of the wiped films and the nip can be treated as semi-infinite slabs in which diffusion is described by

$$\frac{\partial c}{\partial t} = D\frac{\partial^2 c}{\partial^2 \xi_1} \tag{12}$$

for each of the wiped films, and by

$$\frac{\partial \hat{c}}{\partial t} = D\frac{\partial^2 \hat{c}}{\partial^2 \xi_2} \tag{13}$$

for the nip.

The appropriate boundary and initial conditions for a particular solution of Eq. 12 are

$$c = w\rho/M \qquad t = 0 \tag{14}$$

$$c = w_i\rho/M \qquad \xi_1 = 0 \tag{15}$$

$$c = w\rho/M \qquad \xi_1 \to \infty \tag{16}$$

and for Eq. 13 are

$$\hat{c} = w\rho/M \qquad t = 0 \tag{17}$$

$$\hat{c} = w_i\rho/M \qquad \xi_2 = 0 \tag{18}$$

$$\hat{c} = w\rho/M \qquad \xi_2 \to \infty \tag{19}$$

The solutions to Eqs. 12–19 for the wiped films and the nip are respectively given by

$$\frac{cM/\rho - w_i}{w - w_i} = \text{erf}\frac{\xi_1}{\sqrt{4Dt}} \tag{20}$$

$$\frac{\hat{c}M/\rho - w_i}{w - w_i} = \text{erf}\frac{\xi_2}{\sqrt{4Dt}} \tag{21}$$

From Eq. 20 the molar flux at the interface between the wiped film on the barrel wall and the gas phase as any instant in time is given by

$$n_f = -D\frac{\partial c}{\partial \xi_1} = \frac{D(w - w_i)}{\sqrt{\pi Dt}}\frac{\rho}{M} \tag{22}$$

while for the nip this flux is

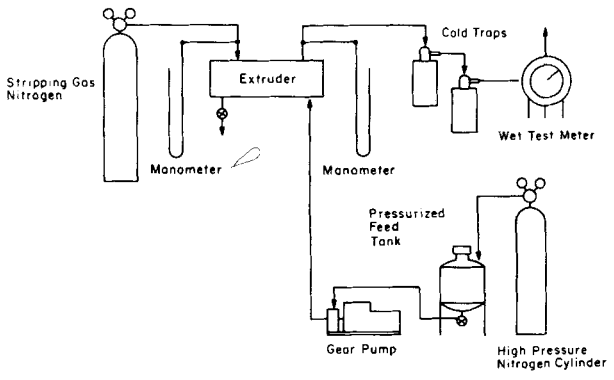

Figure 6. Process flow sheet for experimental studies conducted in this work.

$$n_n = -D\frac{\partial \hat{c}}{\partial \xi_2} = \frac{D(w - w_i)}{\sqrt{\pi Dt}}\frac{\rho}{M} \tag{23}$$

The expression for the molar flux at the surface of the screws, n_{fs}, is identical to Eq. 22. The average molar flux at each of these surfaces is given by

$$N_f = \frac{1}{\theta_f}\int_0^{\theta_f} n_f dt = \frac{2}{\sqrt{\pi}}\sqrt{\frac{D}{\theta_f}}\frac{\rho}{M}(w - w_i)$$

$$N_{fs} = \frac{2}{\sqrt{\pi}}\sqrt{\frac{D}{\theta_{fs}}}\frac{\rho}{M}(w - w_i)$$

and

$$N_n = \frac{1}{\theta_n}\int_0^{\theta_n} n_n dt = \frac{2}{\sqrt{\pi}}\sqrt{\frac{D}{\theta_n}}\frac{\rho}{M}(w - w_i) \tag{25}$$

It is often convenient to express the molar flux for mass transfer in terms of a mass transfer coefficient, and in these circumstances Eq. 10 can be written as

$$N_t a = \frac{\rho}{M}(k_L a)(w - w_i) = N_n a_n + N_f a_f + N_{fs} a_s \tag{26}$$

Substitution of Eqs. 24 and 25 into Eq. 26 results in

$$(k_L a) = \left(\frac{4}{\pi}\frac{D}{\theta_f}\right)^{1/2} a_f + \left(\frac{4}{\pi}\frac{D}{\theta_n}\right)^{1/2} a_n + \left[\frac{4}{\pi}\frac{D}{\theta_{fs}}\right]^{1/2} a_{fs} \tag{27}$$

which can be rearranged to

$$(k_L a) = 2\sqrt{\frac{D}{\pi}\frac{1}{\theta_f}}\, a_b \left(\frac{a_f}{a_b}\right) \times \left[1 + \left(\frac{\theta_f}{\theta_n}\right)^{1/2}\frac{a_n}{a_f} + \left[\frac{\theta_f}{\theta_{fs}}\right]^{1/2}\frac{a_{fs}}{a_f}\right] \tag{28}$$

In the limit when the volume of the nip is negligible in comparison with the total channel volume (i.e., low holdup), Eq. 28 can be simplified. In these circumstances

$$\frac{a_f}{a_b} \approx 1; \quad \frac{a_n}{a_f} \approx 0 \tag{29}$$

and Eq. 28 reduces to

$$k_L a = \frac{2}{\sqrt{\pi}} a_b \left(\frac{D}{\theta_f}\right)^{1/2}\left[1 + \left(\frac{\theta_f}{\theta_{fs}}\right)^{1/2}\frac{a_{fs}}{a_f}\right] \tag{30}$$

In the appendix it is shown that exposure times for the various films are given by

$$\theta_f = \frac{2\pi}{pN}\left[\frac{1}{2} + \frac{p}{\pi}\cos^{-1}\frac{\rho_c}{2}\right]; \quad \theta_{fs} = \frac{2\pi}{N} \tag{31}$$

and therefore Eq. 30 can be written as

$$\frac{k_L a}{a_b} = \frac{2}{\pi}\left[\frac{DpN}{\left(\frac{1}{2} + \frac{p}{\pi}\cos^{-1}\frac{\rho_c}{2}\right)}\right]^{1/2} \times \left[1 + \frac{1}{\sqrt{p}}\left(\frac{1}{2} + \frac{p}{\pi}\cos^{-1}\frac{\rho_c}{2}\right)^{1/2}\frac{a_{fs}}{a_f}\right] \tag{32}$$

which is the working equation for predicting mass transfer rates.

EXPERIMENTAL

A diagram of the process flow sheet for the experiments that were conducted in the course of this study is shown in Figure 6. A polymeric solution of known composition is pumped by a calibrated gear pump from a pressurized feed tank to the inlet port of the twin-screw extruder. A high-pressure nitrogen cylinder, which is also connected to the feed tank, serves to pressurize the liquid in the tank, thus assuring that the inlet to the gear

TABLE 1. EXTRUDER DIMENSIONS AND SCREW GEOMETRY FOR TELEDYNE-READCO "TWO-INCH" TWIN-SCREW PROCESSOR

Screw diameter, D_s, m	$5.08 \cdot 10^{-2}$
Screw length, m	$4.06 \cdot 10^{-1}$
Screw lead, t, m	$4.13 \cdot 10^{-2}$
Channel width, W, m	$2.02 \cdot 10^{-2}$
Channel depth, H, m	$1.14 \cdot 10^{-2}$
Helix angle, ϕ, degrees	12
Flight clearance, δ, m	$2.5 \cdot 10^{-4}$
Centerline distance, C_L, m	$3.89 \cdot 10^{-2}$
Number of screw tips, p	2
Length of devolatilization zone, Z, m	$2.87 \cdot 10^{-1}$
Cross sectional area of empty barrel, S, m^2	$2.00 \cdot 10^{-3}$
Surface area of barrel per unit volume of empty barrel, a_b, m^{-1}	$1.24 \cdot 10^{2}$

pump is filled with solution at all times. The stripped polymeric solution which leaves the extruder is collected, weighed, and retained for analysis of its composition.

The gas used for stripping the volatile component from the polymeric solution is nitrogen, contained in a second pressurized cylinder. The gas can be introduced into the extruder so that it flows either cocurrently or countercurrently relative to the flow of liquid, but in Figure 6 countercurrent flow is shown. The gas stream which discharges from the extruder passes through two cold traps in series where the volalite component in the gas stream is condensed. The total volume of the stripping gas which flows through the extruder is measured by a wet test meter connected to the exit of the cold traps. The average pressure in the gas stream within the devolatilization zone and the gas phase pressure drop over the devolatilization zone are measured by mercury manometers connected to the gas inlet and outlet ports of the extruder.

Equipment

All devolatilization studies were conducted in a laboratory-sized fully intermeshing, corotating twin-screw extruder manufactured by Teledyne-Readco. The extruder barrel used in these studies was fabricated from poly(methyl-methacrylate), which is transparent; this permitted making visual observations as to whether bubbles were present within the liquid in the devolatilization zone. In addition, the exact length of the devolatilization zone could also be measured. Table 1 lists the important characteristics of the extruder and barrel.

A 6 gal (22.7 L) steel tank was used as the solution feed tank for the system and was pressurized under nitrogen while experiments were run. The gas cylinder was connected to the tank with 1/4 in. (6.4 mm) Swagelok fittings and 1/4 in. polyethylene tubing. High pressures were necessary to insure that the inlet to the gear pump was filled with liquid at all times. The outlet from the feed tank was regulated by a 1/2 in. (12.7 mm) ball valve which in turn was connected to 1/2 in. stainless steel tubing that led to the gear pump. The gear pump (Model BPB-4391) was manufactured by Zenith and was driven by a Graham variable speed transmission. The discharge of the gear pump was connected to a tee, one side of which was connected to the feed port of the extruder by 1 in. (25.4 mm), 304 stainless steel tubing. The second side of the tee was connected to a 1/2 in. ball valve which was used to collect samples of the feed so that its exact composition could be determined. A calibration curve relating the mass throughput rate of the gear pump to its rotational speed was prepared so that desired mass flow rates of solution through the extruder could be obtained approximately by adjusting the rotational speed of the gear pump. The calibration procedure was straightforward and simply involved weighing the output from the gear pump over a given period of time at a known rotational speed of the gear pump. For these measurements undiluted polybutene was used. Mass flow rates were then converted to volumetric flow rates using the polymer density.

The flow of the nitrogen stripping gas was regulated by a standard nitrogen pressure regulator, but precise measurement of the gas flow rate was made using a wet test meter. Connections between the cylinder containing the stripping gas and the inlet port of the extruder were made with 1/4 in. (6.4 mm) Swagelok fittings and 1/4 in. polyethylene tubing. The two cold traps used to condense and collect the volatile component from the

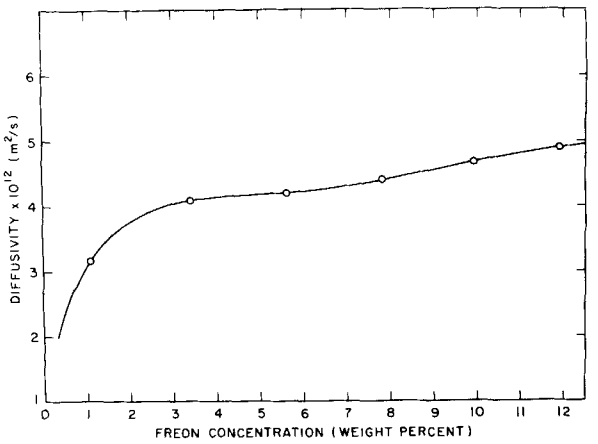

Figure 7. Diffusion coefficient as a function of concentration for freon/polybutene solutions at $T = 25°C$ (after Secor, 1967).

gas stream were obtained from the Ace Glass Corporation. These traps contained 5 mm glass bead packing and provided the necessary surface area for condensing the volatile component. Each cold trap was cooled by liquid nitrogen in a 1,040 ml Aladdin cryogenic Dewar flask. The vapor-free nitrogen stream was then passed through a Precision Scientific wet test meter which accurately measured the flow of nitrogen through the extruder. Connections between the extruder, the cold traps, and the wet test meter were made with 3/8 in. (9.5 mm) Tygon tubing.

Temperatures of the inlet and outlet streams to the extruder were measured using two Thermo Electric iron-constantan thermocouples, Model No. 11235, and an Omega LED digital thermometer, Model 199 JF. All pressures and pressure differences were measured using standard U-tube mercury manometers.

Material Properties and Characterization

The polymeric solutions used in these studies were polybutene-freon mixtures which contained less than about 5 wt% freon. The polybutene used is designated Polybutene-32. It is a clear Newtonian liquid having a viscosity of 1,000 poise (100 Pa·s) at 25°C, and is supplied by the Chevron Chemical Co. (Chevron, 1980). The volatile component in the polmeric solution is commercially known as Freon-113 (1,1,2-trichloro-2,2,1-trifluoroethane, du Pont, 1978).

The concentration of both the inlet and outlet solutions to the extruder was determined from refractive index measurements using a Bausch and Lomb ABBE L refractometer. This determination requires the use of a calibration curve which was obtained by measuring the refractive index of freon-polybutene solutions of known concentration. This curve was found to be linear over the range of 0 to 10 wt% freon.

Two additional physical properties of the solution must be known in studies of the type reported here; these are the molecular diffusivity and solubility of Freon-113 in Polybutene-32. Values for the molecular diffusivity as a function of concentration have previously been measured by Secor (1967); these data are shown in Figure 7.

The solubility of Freon-113 in Polybutene-32 was determined experimentally using gas-liquid chromatography as described by Newman and Prausnitz (1972, 1973). For the range of concentrations of freon in polybutene considered in this study, the solubility relationship can be described by Henry's law in the form

$$P = H_F w \tag{33}$$

where H_F is a weight-fraction-based Henry's constant. The values for Henry's constant that we obtained experimentally as a function of temperature were used to prepare an Arrhenius plot from which we determined the heat of vaporization of Freon-113 to be 6,584 cal/mol (appendix). This value compares favorably with the liteature value of 6,571 cal/mol (Dean, 1979), thus leading us to conclude that our procedure for determining Henry's contant did not result in significant errors. Complete details of this procedure are given by Collins (1982).

Procedure

A solution of Polybutene-32 and Freon-113 of the desired concentration was prepared by mixing the components in a 5 gal (18.9) container. The container was then sealed for two days so that air bubbles formed during the mixing process could escape. The solution was then transferred to the holding tank where the solution again sat for a period of two days so that air bubbles formed due to this transfer could escape. The liquid was then pressurized with nitrogen to 100 psig (689 kPa).

Several measurements were taken prior to the start of the experiment; these included:

1. Measurement of the weight of each cold trap including the glass bead packing.
2. Measurement of the weight of the container used to collect the solution from the outlet of the extruder.
3. Measurement of the barometric pressure.

The rotational speed of the screw and the gear pump were set to the desired values with the use of a stroboscope. Once the liquid began to collect within the barrel, the valve on the exit stream from the extruder was adjusted to maintain a back-up length of liquid in the barrel at approximately 0.06 m. The flow rate of the stripping gas was determined by measuring the time required to pass a given volume of gas through the extruder and the wet test meter. The nitrogen regulator on the gas cylinder was then adjusted until the desired flow rate was obtained. After a constant gas flow rate was obtained, an additional five minutes was allowed to elapse to insure that steady state had been reached. The Dewar flasks were then filled with liquid nitrogen and placed in position. The gas stream was then disconnected from the wet test meter and the meter reset to zero.

Approximately one minute before the experiment was actually begun the cold traps were placed in the Dewar flasks, which contained the liquid nitrogen so that thermal equilibrium could be reached. Styrofoam was used to seal the Dewars and retard evaporation, but because some evaporation did occur a small amount of liquid nitrogen needed to be added to the Dewars every few minutes to keep the traps completely submersed. The cold traps were then connected in series with the wet test meter with Tygon tubing.

At the start of each run the gas stream which discharges from the extruder was connected to the first cold trap in the series and collection of the condensed solvent vapors was begun. During the run the gauge pressure in both manometers and the temperature of the liquid feed and outlet streams were monitored and recorded continuously. In addition, the temperature of the water in the wet test meter and the pressure within its vapor space were recorded so that the gas flow rate could be corrected to standard conditions of 0°C and 1 atm (101.3 kPa) for which the meter was calibrated. All experiments were run for approximately 20 min.

At the conclusion of the experiment the elapsed time was noted using a precision timer, the cold traps were disconnected from both the wet test meter and the extruder, and each of the cold traps was then weighed. The liquid flow rate, the gas flow rate, and the screw rotational speed were maintained at their set values until liquid samples could be collected from the outlet of the extruder and the melt pump. The samples were collected in four dram sample vials that were completely filled so that a space did not exist into which the freon could evaporate. These samples were used to determine the compositions of the inlet and outlet streams. The final reading on the wet test meter and the total weight of liquid collected from the barrel outlet over the time interval of the experiments were recorded.

Between successive runs the cold traps were cleaned to prevent excessive buildup of freon within the traps which would otherwise decrease their efficiency. Also, the disassembled components of both traps were heated to 100°C in an oven for approximately twenty minutes.

Data Reduction

The equipment design and experimental procedure were developed so that a direct measurement could be made of K_La, the product of the overall mass transfer coefficient and the interfacial area per unit volume of extruder. In terms of experimentally measured variables K_La is given by

$$K_La = \frac{\dot{m}M}{(w - w^*)_{lm}SZ\rho} \tag{34}$$

where $\dot{m}$ is the average molar rate of devolatilization of the volatile component, $(w - w^*)_{lm}$ is the logarithmic mean concentration driving force

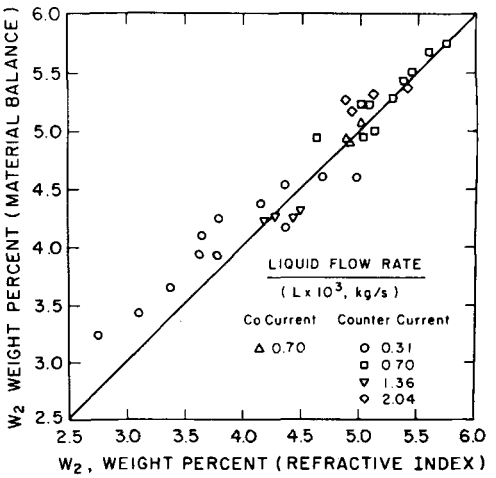

Figure 8. Concentration of freon in the exit stream from extruder as determined by refractive index and by material balance; symbols reflect differences in liquid flow rate and whether gas flow is cocurrent or countercurrent.

$$(w - w^*)_{lm} = \frac{(w - w^*)_2 - (w - w^*)_1}{\ln \dfrac{(w - w^*)_2}{(w - w^*)_1}} \tag{35}$$

and SZ is the total volume within the devolatilization zone.

The value of $\dot{m}$ was obtained from a knowledge of the mass of freon condensed and collected in the cold traps over a known time interval. The mass fraction of freon in the feed stream, w_1, was determined by measuring the refractive index of a sample taken from the feed stream. The mass fraction of freon in the exit stream, w_2, was determined by direct measurement of the refractive index of samples of the exit stream, and also by making a solvent balance around the extruder which results in

$$w_2 = \frac{L_1w_1 - \dot{m}M}{L_1 - \dot{m}M} \tag{36}$$

Figure 8 is a plot of the results obtained by the two methods for several experiments and shows that the two methods give essentially identical results. In this work w_2 was determined using Eq. 36.

When the flow of stripping gas is countercurrent to the flow of liquid in the extruder, as was the case in most of the experiments conducted here, w_2^* is identically zero since the stripping gas is pure nitrogen. The value of w_1^* is computed from Eq. 37.

$$w_1^* = \frac{P_T}{H_F}\left(\frac{\dot{m}}{G' + \dot{m}}\right) \tag{37}$$

RESULTS AND DISCUSSION

The interphase mass transfer process which occurs when freon is extracted from polybutene-freon solutions involves diffusion through two resistances in series: the resistance to mass transfer in the liquid phase and the resistance in the gas phase. In mathematical terms, the mass transfer rate in each of these phases is given by

$$\dot{m} = (k_La)\frac{\rho}{M}(w - w_i)_{lm}SZ = k_Ga P_T(y_i - y)SZ \tag{38}$$

or, in terms of an overall liquid phase mass transfer coefficient,

$$\dot{m} = (K_La)(w - w^*)_{lm}\frac{\rho}{M}SZ \tag{39}$$

In circumstances when the equilibrium relationship is linear, Eqs. 33, 38, and 39 can be combined to yield

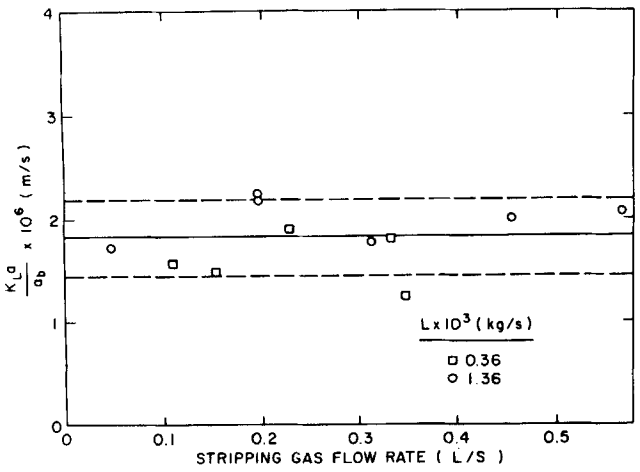

Figure 9. Influence of flow rate of stripping gas on overall liquid phase mass transfer coefficient; the dashed lines reflect ± 20% deviation from solid line as determined by linear regression. Gas flow was countercurrent, screw speed is 5.12 rad/s.

$$\frac{1}{K_L a} = \frac{1}{k_L a} + \frac{S}{M H_F k_G a} \tag{40}$$

where the first term on the righthand side reflects the resistance to mass transfer in the liquid phase and the second term reflects that in the gas phase. When the liquid phase resistance is controlling, Eq. 40 reduces to

$$K_L a = k_L a \tag{41}$$

which means that the individual liquid phase mass transfer coefficient can be determined simply by measuring the overall liquid phase mass transfer coefficient.

The first set of experiments that we conducted was designed to determine whether the liquid phase resistance was the controlling resistance. Since the magnitude of the gas phase resistance is known to vary with the flow rate of the stripping gas, experiments were conducted in which the gas flow rate was varied over a wide range of values when the screw speed and liquid flow rate were held constant.

Figure 9 is a plot of measured values for the product of the overall liquid phase mass transfer coefficient and the surface area for mass transfer, divided by the known value for the barrel surface area. Since the surface area for mass transfer probably does not vary significantly over the range of liquid flow rates considered, this figure is essentially a plot of the overall liquid phase mass transfer coefficient. The data are well represented by a horizontal line to within ±20%, and we can thus conclude that the resistance to mass transfer in the gas phase is small in comparison to that of the liquid phase. Consequently, the individual liquid phase mass transfer coefficient can be determined directly from the measured values for the overall liquid phase mass transfer coefficient.

Figure 10 is a plot which shows how the product of the liquid phase mass transfer coefficient and the surface area per unit volume varies with screw speed for a wide range of liquid flow rates when the flow of stripping gas is both cocurrent and countercurrent. Note that as in Figure 9 the ordinate in this figure is $(k_L a)/a_b$. The solid line drawn through the data points was determined by linear regression and is given by

$$\frac{k_L a}{a_b} = 7.3 \cdot 10^{-7} N^{1/2} (k_L \equiv m/s, N \equiv s^{-1}) \tag{42}$$

The theoretical prediction, Eq. 32, reduces to

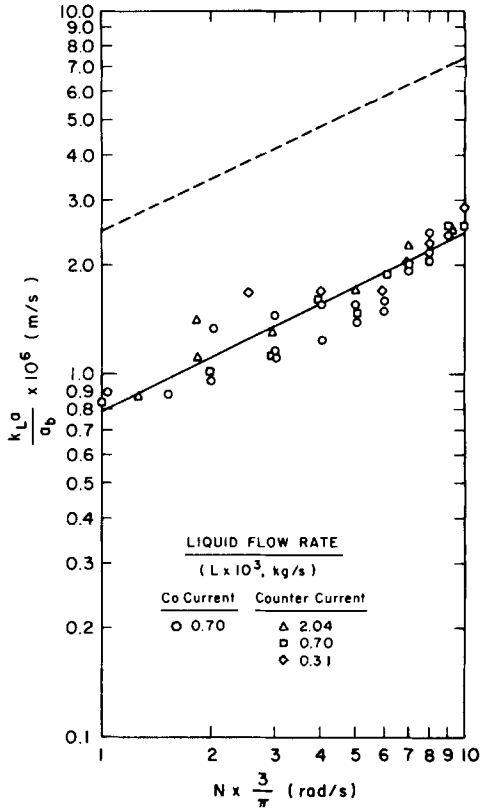

Figure 10. Comparison of measured liquid phase mass transfer coefficients with predictions from penetration theory. - - - plot of Eq. 43 with $D = 4.2\ 10^{-12}$ m²/s (Secor, 1967); —— plot determined by linear regression, described by Eq. 42. Experimentally determined values of $k_L a$ were divided by a_b from Table 1 to obtain a consistent comparison with theory.

$$\frac{k_L a}{a_b} = 2.3 \cdot 10^{-6} N^{1/2} \tag{43}$$

for the conditions employed in this study. The dependence of $k_L a/a_b$ on screw speed is correctly predicted, but the predicted values for $k_L a/a_b$ differ by roughly a factor of three.

Two reasons can be cited toward explaining this difference. First, the assumption that the surface area of the film on the barrel wall is equal to the surface area of the barrel wall may be incorrect. And second, the assumption that the surface area of the film on the screws and the surface area of the film on the barrel wall are equal may also be incorrect. If conditions are such that only 10% of the barrel wall is covered by a film of polymer, an order-of-magnitude difference can result between the theoretical prediction and the experimental results for $k_L a/a_b$ since $a_f/a_b = 0.10$. Coverages of the barrel wall of this magnitude would most likely occur in circumstances when the holdup is uncommonly low (less than 10% of the free volume). Throughout the course of this study, the holdup was estimated to be in the range of 5 to 10%, and this could account for the observed difference between theory and experiment.

The assumption that the surface area of the film on the screws is nearly equal to the surface area of the film on the barrel wall is judged to be correct and should not significantly affect the theoretical predictions. It seems reasonable to expect that the polymeric solution would wet the surfaces of the screws to about the same degree that it would wet the surface of the barrel wall, and since the surface area of the screws is nearly equal to that of the barrel wall, the ratio a_{fs}/a_f should be close to unity.

ACKNOWLEDGEMENT

We wish to thank Teledyne, Inc., and Teledyne-Readco for their financial support and technical advice throughout the course of this research.

APPENDIX A

In the limit when the degree-of-fill in the channel is zero, an expression for the film exposure time θ_f can be derived by noting from Figure 5 that

$$\theta_f = \frac{(W - x')}{V_{Bx}} \tag{A1}$$

$$\theta_f \cong \frac{W}{V_{Bx}} \qquad x' \to 0 \tag{A2}$$

But, from Eqs. 4, 6, and 7 we have

$$W = \frac{t_s \cos\phi}{p} - e \tag{4}$$

$$e = \frac{t_s\, \alpha \cos\phi}{2\pi} \tag{6}$$

$$\alpha = \frac{\pi}{p} - 2\cos^{-1}\frac{\rho_c}{2} \tag{7}$$

and therefore

$$\theta_f \cong \frac{1}{V_{Bx}}\left[\frac{t_s\cos\phi}{p} - \frac{t_s\cos\phi}{2\pi}\left(\frac{\pi}{p} - 2\cos^{-1}\frac{\rho_c}{2}\right)\right] \tag{A3}$$

If we now substitute Eq. 5

$$t_s = \pi D_s \tan\phi \tag{5}$$

into Eq. A3, we obtain

$$\theta_f = \frac{\pi D_s \sin\phi}{V_{Bx}}\left[\frac{1}{p} - \frac{1}{2\pi}\left(\frac{\pi}{p} - 2\cos^{-1}\frac{\rho_c}{2}\right)\right] \tag{A4}$$

which, for $V_{Bx} = \pi D_s N \sin\phi$,

$$\theta_f = \frac{2\pi}{pN}\left[\frac{1}{2} + \frac{P}{\pi}\cos^{-1}\frac{\rho_c}{2}\right] \tag{A5}$$

APPENDIX B

The correctness of the values of Henry's constants obtained by gas-liquid chromatography can be verified by considering the Clausius-Clapeyron equation:

$$\ln\frac{P_2^o}{P_1^o} = \frac{\Delta H_v}{R}\left[\frac{1}{T_1} - \frac{1}{T_2}\right] \tag{B1}$$

where P_i^o is the vapor pressure of the pure volatile component at temperature T_i. For ideal gas phase the equilibrium partial pressure P over a solution containing W wt% of the volatile component is given by:

$$p = \gamma P^o w \tag{B2}$$

where γ is a weight-fraction based activity coefficient. Henry's law applies when W is sufficiently small for γ to be approximated by its infinite dilution value:

$$\gamma \simeq \lim_{w\to 0}\gamma = \gamma_\infty \tag{B3}$$

in which case the Henry's law constant H_F is given by:

$$H_F = \gamma_\infty P^o \tag{B4}$$

Substitution of Eqs. B3 and B4 into Eq. B2 yields Eq. 33. Since activity coefficients are known to be weak functions of temperature, combination of Eqs. B1 and B4 yields:

$$\ln\frac{H_{F2}}{H_{F1}} = \frac{\Delta H_v}{R}\left[\frac{1}{T_1} - \frac{1}{T_2}\right] \tag{B5}$$

Equation B-5 shows that an Arrhneius plot of H_f should yield the value of the heat of vaporization of the volatile component.

NOTATION

a	= effective surface area for mass transfer per unit volume of empty extruder barrel
a_b	= surface area of the extruder barrel per unit volume of empty extruder
a_f	= interfacial area of the wiped film on the barrel wall per unit volume of empty extruder
a_{fs}	= interfacial area of wiped film on the surface of the screws per unit volume of empty extruder
a_n	= interfacial area of the nip per unit volume of empty extruder
c	= concentration of volatile species
$\hat{c}$	= concentration
C_L	= centerline distance between screws
D	= molecular diffusivity
D_s	= screw diameter
e	= width of flight tips
G'	= solvent-free molar flow rate of gas stream
h	= local depth of screw channel
H	= maximum depth of screw channel
H_F	= Henry's constant for freon in polybutene
ΔH_v	= heat of vaporization
k_L	= liquid phase mass transfer coefficient
K_L	= overall liquid phase mass transfer coefficient
L	= mass flow rate of liquid
L_1	= mass flow rate of liquid at inlet to extruder
M	= molecular weight of volatile component
n_f	= instantaneous molar flux from film
n_{fs}	= instantaneous molar flux from film on the surface of the screws
n_n	= instantaneous molar flux from nip
N	= screw speed
N_f	= average molar flux from wiped film on the surface of the barrel wall
N_{fs}	= average molar flux from wiped film on the surface of the screws
N_n	= average molar flux from nip
N_t	= total molar flux
p	= number of screw tips
P	= partial pressure of volatile component
P_T	= pressure in the gas phase
R	= gas constant
R_s	= screw radius
S	= cross-sectional area of empty barrel
t	= time
t_s	= lead of screw element
T_1, T_2	= temperature
V_{Bz}	= down-channel component of barrel velocity
V_{Bx}	= cross-channel component of barrel velocity
w	= weight fraction of volatile component in liquid phase
w_1	= weight fraction of volatile component in liquid at inlet of extruder
w_2	= weight fraction of volatile component in liquid at outlet of extruder
w_i	= weight fraction of volatile component at liquid-vapor interface

w^* = weight fraction in equilibrium with the local gas-phase composition
W = maximum channel width
x = coordinate
x' = coordinate
y = mole fraction in gas
y_i = mole fraction in gas stream at vapor-liquid interface
Z = length of devolatilization zone
z = coordinate

Greek Letters

α = tip angle
γ = activity coefficient based on weight fraction
δ = clearance between flight tip and barrel
θ_f = exposure time of wiped film
θ_n = exposure time of nip surface
ξ_1 = coordinate direction perpendicular to surface of wiped film
ξ_2 = coordinate direction perpendicular to surface of nip
ρ = polymer solution density
ρ_c = ratio of centerline distance between screws to barrel radius
ϕ = helix angle

LITERATURE CITED

Biesenberger, J. A., "Polymer Devolatilization: Theory of Equipment," *Poly. Eng. Sci.*, **20**, 1,015 (1980.

Chevron, "Chevron Polybutenes: Compounds for Your Imagination," Chevron Chemical Co., San Francisco (1980).

Collins, G. P., "Devolatilization of Polymeric Solutions in an Intermeshing Co-Rotating Twin-Screw Extruder," M.S. Thesis, Univ. of Delaware (1982).

Coughlin, R. W., and G. P. Canveri, "Drying Polymers During Screw Extrusion," *AIChEJ.*, **15**, 560 (1969).

Dean, J. A., ed., *Lange's Handbook of Chemistry*, 12th ed., McGraw-Hill, New York (1979).

du Pont de Nemours Co., E.I., Bulletin B-2 (1978).

Hess, M., and K. Eise, *Soc. Plast. Eng.*, Technical Papers, **23** (1977).

Hwang, B. K., "Fluid Flow Studies in Twin-Screw Extruder," Ph.D. Dissertation, Univ. of Delaware (1982).

Latinen, G. A., "Devolatilization of Viscous Polymer Systems," *ACS Adv. Chem. Series*, **34**, 235 (1962).

Moffatt, H. K., "Viscous and Resistive Eddies Near a Sharp Corner," *J. Fluid Mech.*, **18**, 1 (1964).

Newman, R. D., and J. M. Prausnitz, "Polymer-Solvent Interactions from Gas-Liquid Partition Chromatography," *J. Phys. Chem.*, **76**, 1,492 (1972).

———, "Thermodynamics of Concentrated Polymer Solutions Containing Polyethylene, Polyisobutylene, and Copolymers of Ethylene with Vinyl Acetate and Propylene," *AIChE J.*, **19**, 704 (1973).

Odian. G., *Principles of Polymerization*, McGraw-Hill, New York (1970.

Roberts, G. W., "A Surface Renewal Model From the Drying of Polymers During Screw Extrusion," *AIChE J.*, **16**, 878 (1970.

Rothe, J., "Devolatilization During Injection Molding," *Devolatilization of Plastic*, Verrin Deutscher Ingenieure Dusseldorf, UDI-Gessellschaft Konststofftechnik (1980).

Secor, R. M., "Diffusion Coefficients in a Halocarbon-Polybutene System," *J. Polym. Sci.*, **5**, 323 (1967).

Todd, D. B., "Polymer Devolatilization," *Soc. Plast. Eng.*, Technical Papers, **20** (1974).

Wener, H., "Devolatilization of Polymers in Multi-Screw Devolatilizers," *Devolatilization of Plastics*, Verrin Deutscher Ingenieure Dusseldorf, UDI-Gessellschaft Kunststoftechnik (1980).

Manuscript received Nov. 30, 1982; revision received Apr. 9, 1984, and accepted Apr. 30.